Photoconductivity of sexithiophene single crystals

Gilles Horowitz,* Fayçal Kouki, and Pierre Valat
Laboratoire des Matériaux Moléculaires, CNRS, 2 rue Henry-Dunant, 94320 Thiais, France

Philippe Delannoy and Joseph Roussel
Groupe de Physique des Solides, Universités Paris 6 et Paris 7, 75251 Paris cedex 05, France
(Received 10 June 1998; revised manuscript received 20 January 1999)

Time-resolved and steady state photoconductivity measurements were carried out on sexithiophene single crystals. We used a surface geometry, where two gold electrodes separated by 2 mm were deposited on the same side of the crystal. Time resolved measurements revealed fast and slow components. The first one, whose decay time is lower than 1 ns, is attributed to the conversion of charge transfer excitons into molecular excitons. The slow component behaves as a second order process, which is analyzed as bimolecular recombination of electrons and holes. It is preceded by an intermediate component that we tentatively ascribe to geminate recombination of the excitons. A similar analysis is used to rationalize the steady-state photocurrent. We find a quantum efficiency of around 10^{-4}. The coincidence between the photoluminescence and photocurrent action spectra, together with the low electric field applied over the crystal, suggest charge generation to occur via thermally activated splitting of molecular excitons. From the quantum efficiency at room temperature, the exciton binding energy is estimated to 0.50 ± 0.06 eV. This value is confirmed by the temperature dependent photocurrent. [S0163-1829(99)01316-8]

INTRODUCTION

The mechanism of photocarrier generation in conjugated polymers and oligomers is currently a highly controversial issue. Basically, two main approaches are in competition. From the classical viewpoint of molecular physics,[1,2] the absorption of light results in the formation of molecular excitons, the binding energy of which is typically 1 eV. For this reason, intrinsic photoconductivity only occurs at incident light energies of at least 1 eV above the optical absorption edge. It can also turn out through an extrinsic process, for instance charge detrapping near a metal electrode, in which case the photocurrent action spectrum would coincide with the absorption spectrum of the molecular material. In the second description,[3] the electronic structure of a conjugated molecule is described in terms of a tight-binding model, where photoexcitations across the band gap create free carriers, as in conventional inorganic semiconductors. In fact, these apparently contradictory pictures correspond to the two extreme cases of the strongly bound Frenkel and large Wannier-Mott exciton, respectively. A general presentation of the controversy can be found in a recent book edited by N. S. Sariciftci (see Ref. 3).

Although photoconductivity is the tool of choice for studying photocarrier generation, their analysis is intricate for many reasons. First, one has to distinguish intrinsic and extrinsic phenomena.[4] Next, the mechanism of carrier generation is coupled with that of charge transport,[5] so that it is not always possible to clearly separate dependencies pertaining to each process. In this respect, it is often of interest to conduct simultaneous time-resolved and steady-state measurements. Finally, measurements are most often carried out on polymeric materials, where effects due to disorder, such as trapping of charge carriers, may hide the intrinsic phenomena.

Sexithiophene ($6T$) is a conjugated oligomer formed by linking six thiophene molecules at α position. Its chemical structure is given in Fig. 1. In the solid state, the molecule presents an all-*trans*, perfectly coplanar geometry, which can therefore be viewed as a rigid rod. Sexithiophene is at present one of the most widely used model molecules of conjugated polymers. One of its major advantages is the access to single crystals,[6] where the number of structural defects is much lower than in polymers or polycrystalline films. The crystal structure of sexithiophene, where the molecules arrange themselves in parallel layers of nearly vertical rods, is shown in Fig. 2. Recent spectroscopic measurements on $6T$ single crystals have greatly clarified the description of its excitonic levels. Low-temperature polarized photoluminescence (PL) allowed Muccini and co-workers[7] to identify the lowest singlet exciton level 18 350 cm^{-1} (2.28 eV) above the ground level. This level belongs to the A_u representation, and because the polarization of the transition is almost perpendicular to the transition dipolar momentum, its oscillator strength is very weak, which explains why this transition is almost impossible to detect in polycrystalline films. Furthermore, the extended states of $6T$, which are not accessible to optical measurements, have been studied by electroabsorption.[8] Features that appear at energies higher than the exciton transition were attributed to a charge-transfer exciton (CTE) located 2.78 eV above ground level, leading to an exciton binding energy of around 0.5 eV. (In a charge-transfer exciton, the plus and minus charges are separated on adjacent molecules. CTE's are also called polaron pairs.)

In the present paper, we report on time-resolved and steady-state photoconductivity measurements on sexithiophene single crystals. We adopted a planar geometry, in which the electrodes are deposited on the same side of the flat crystal, which differ from the most generally used sandwich structure, where the electrodes are deposited at both

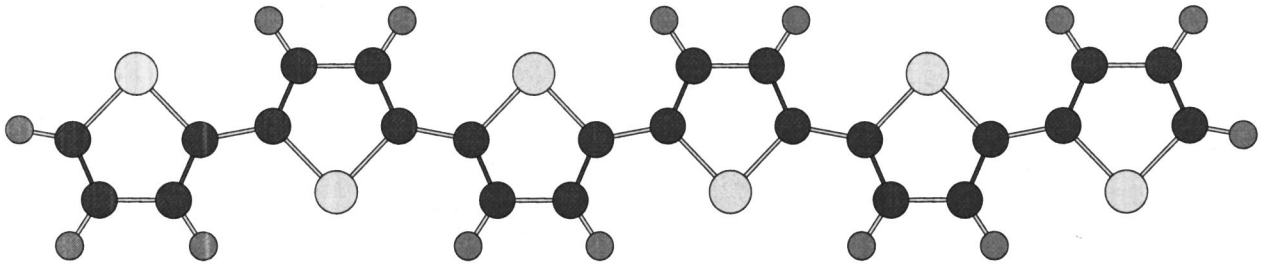

FIG. 1. Chemical structure of sexithiophene.

sides of a thin film. By using a large electrode distance (2 mm), we were able to illuminate the crystal far from the electrodes, thus avoiding extrinsic photogeneration. A model involving bimolecular recombination of the photogenerated carriers is used to analyze both the steady state and the long-lived time-resolved photocurrent. From the quantum efficiency of carrier generation, we deduce that the exciton binding energy is around 0.5 eV, in good agreement with previous estimations. The magnitude of the binding energy is also confirmed by temperature-dependent measurements of the photocurrent.

EXPERIMENT

Sexithiophene single crystals where grown from the vapor phase in a home-made vertical evaporator,[6] which consists of a 5-cm-diam glass tube, round closed at one end and fitted at the other to a gas stopcock. The powdered material was disposed at the bottom of the tube, and the crystals collected on a glass rod equipped with an appropriate collector and placed at the center of the tube. The tube was introduced in a vertical furnace, with the collector slightly above the inner rim of the furnace. The growth was conducted under argon reduced pressure (~500 Pa), at a temperature of 210 °C. The crystals, which appear as thin (around 10 μm) orange plates with lateral dimensions up to 5 mm, were picked up from the collector after one or two days.

For photoconductivity measurements, flat crystals were selected and carefully deposited on 0.2-mm-thick alumina plates, on which they spontaneously adhered. Two gold strips (thickness of 50 nm, width of 1 mm, separated by 2 mm) were then vacuum-evaporated on the crystal. The measurement setup is described in Fig. 3. The crystal is polarized with a voltage source, and the current measured through a load resistance ranging between 50 Ω and 1 MΩ, which in all cases is much smaller than the crystal series resistance. The voltage detector was a lock-in amplifier (ATNE) for steady state, and a fast oscilloscope (Tektronik TDS 620) for time-resolved measurements. The light source consisted of a Xe arc lamp, equipped with a chopper, for steady-state measurements, and a N_2 laser (337 nm) for the time-resolved photoconductivity. Quartz lenses were used to adjust the light spot to the crystal size. Light illumination was estimated with a calibrated silicon photodiode (UDT), and was adjusted with neutral density filters. Spectral response was obtained with the help of a grating monochromator (Jobin Yvon). Temperature-dependent measurements were done by placing the mounted crystal on the cold finger of an Air Product close-cycle cryostat. The temperature was measured with a H chromel/Au-Fe thermocouple and monitored with a temperature controller. Finally, photoluminescence measurements were carried out on a spectrofluorimeter (SLM).

RESULTS

Time-resolved measurements

In a typical time-resolved measurement, the crystal is first polarized at a constant voltage. Then, a short laser pulse (337 nm, 0.4 ns) is directed on the surface of the crystal, and the resulting photocurrent recorded on a fast oscilloscope. A lens was used to concentrate the light between the gold electrodes. In the curve given in Fig. 4, we used a cylindrical lens and the light was spread all over the area comprised between the electrodes. The voltage is 1000 V, which corresponds to a field of 5000 V/cm if we assume a uniform field all along the crystal, and the load resistance 1 kΩ. We note that the current decrease is not exponential, as shown in the inset of the figure.

If we now use a load resistance of 50 Ω (this is actually the input resistance of the oscilloscope), and concentrate the

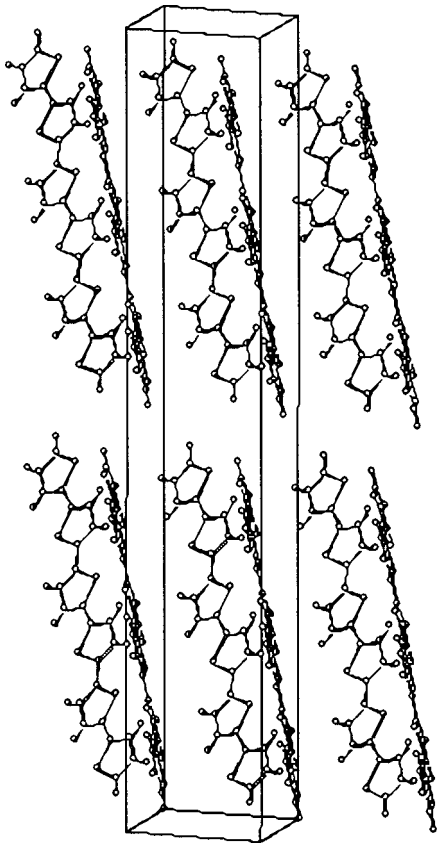

FIG. 2. Crystal structure of sexithiophene.

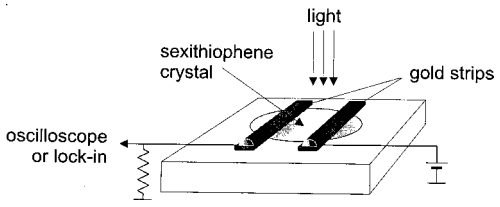

FIG. 3. Experimental setup for photoconductivity measurements. The flat crystal is deposited on an alumina substrate, and two vacuum evaporated gold strips act as electrical contacts.

light to a very small spot with a spherical lens, we get the much shorter response given by Fig. 5. In this case, the voltage is again 1000 V. The rise and decay times (around 1 ns) correspond to the instrumental limit of our oscilloscope. We note that recent picosecond time-resolved measurements on poly(phenylene-vinylene) (PPV) (Ref. 9) have revealed a similar fast response, with an initial decay time of about 100 ps.

Steady-state photoconductivity

The steady-state photocurrent was measured under chopped light, at a frequency of 80 Hz, with a load resistance of 1 MΩ. Higher chopping frequencies lead to a lowering of the signal, due to the high load resistance. The voltage applied to the electrodes was 300 V.

The action spectrum, corrected for the incident light fluctuations, is given in Fig. 6. Also shown on the same figure is the photoluminescence excitation spectrum measured on the same crystal.

The variation of the steady-state photocurrent as a function of the incident photon flux is shown in Fig. 7. The incident light is monochromatic (510 nm). The dependence is linear at low intensities, but tends to become sublinear at higher intensities. The solid curve is a least-squares fit to the model that will be developed in the next section.

Finally, Fig. 8 shows the temperature dependence of the photocurrent. The data were recorded under monochromatic light (530 nm). The temperature-dependent mobility measured on a field-effect transistor constructed on a $6T$ single crystal is also shown. Note that the magnitude of the mobility is slightly lower than that reported earlier,[10,11] which may be due to problems of contact resistance.

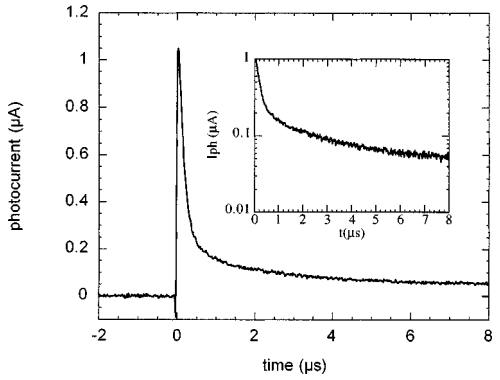

FIG. 4. Time-resolved photoconductivity of a sexithiophene crystal. The light pulse was given by a N_2 laser (337 nm, 0.4 ns). Light was spread all over the area comprised between the gold electrodes (see Fig. 1), with the help of a quartz cylindrical lens. Load resistance: 1 kΩ. A linear-log plot of the photocurrent decay is shown in the inset.

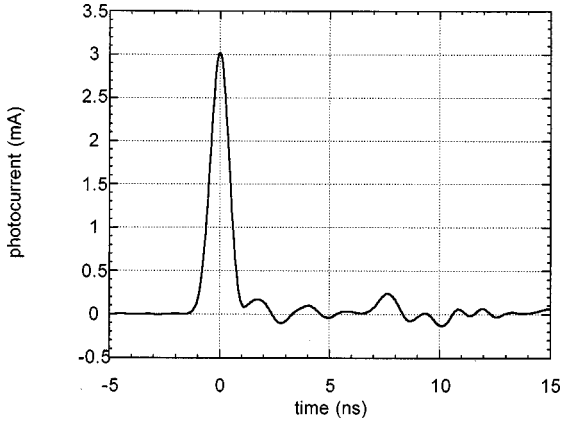

FIG. 5. Same as Fig. 4, with a load resistance of 50 Ω. This time, the light is concentrated on a small point with a spherical lens.

DISCUSSION

We shall first focus on the slow decay (Fig. 4). The curve can be divided into two components. The first one (which lasts less than half a microsecond) is most likely widened by the large load resistance needed to detect the weak photocurrent. We shall come back later to this first component, and will first discuss the second component. The linear-log plot of the curve (inset in Fig. 4) convinces us that this is not an exponential decay. This indicates that unlike in disordered materials such as polycrystalline or polymeric films, charge transport is not limited by traps. We will therefore model the decay by means of bimolecular recombination of electrons and holes. The general model is depicted by Eq. (1), where n is the density of photogenerated carriers (electrons and holes) generated at an equivalent rate G, and n_0 is the equilibrium density of majority carriers (holes in the case of sexithiophene),

$$\frac{\partial n}{\partial t} = G - \gamma(n_0 + n)n. \tag{1}$$

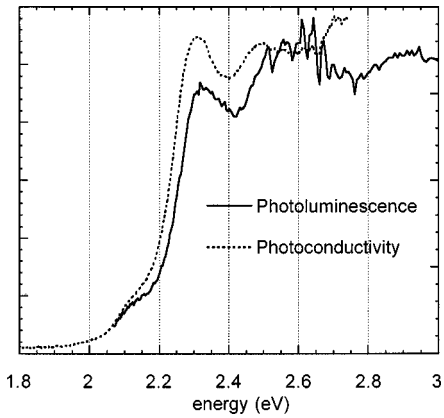

FIG. 6. Photocurrent action spectrum of a sexithiophene single crystal, along with the photoluminescence excitation spectrum measured on the same crystal.

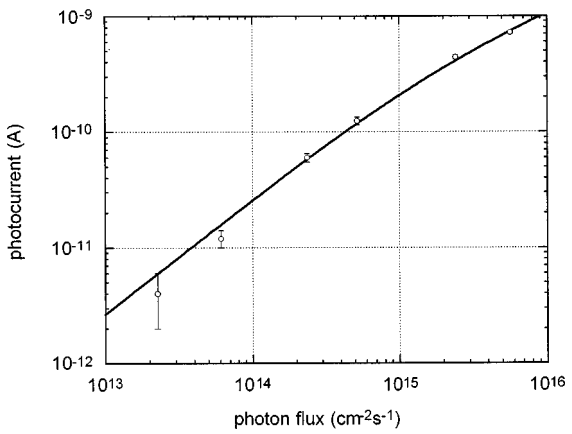

FIG. 7. Variation of the steady-state photocurrent as a function of the incident photon flux, measure under monochromatic light at 510 nm.

γ is the bimolecular recombination coefficient. The time-resolved response is obtained by stating $G=0$ in Eq. (1). The general solution reads

$$n=n_0\left(\frac{n_0+n(0)}{n(0)}\exp(\gamma n_0 t)-1\right)^{-1}. \tag{2}$$

Here, $n(0)$ is the density of photocarriers at $t=0$. At short time ($\gamma n_0 t \ll 1$) and strong illumination [$n(0) \gg n_0$], Eq. (2) reduces to

$$\frac{1}{n}=\frac{1}{n(0)}+\gamma t. \tag{3}$$

The total photocurrent I_{ph} is the sum of currents of positive and negative charges. As both species are generated at equal rate, I_{ph} is given by the density of photogenerated carriers times the sum of the mobility of each kind of carrier. The result is given by Eq. (4), where W is the length of the electrodes and d_{eff} is the effective thickness of the photogenerated charge distribution,

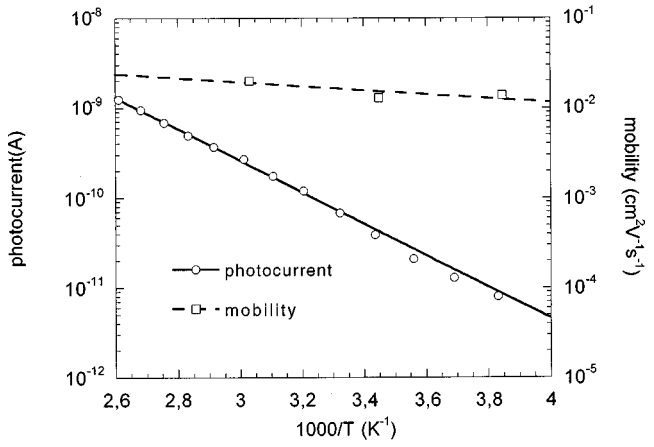

FIG. 8. Temperature dependence of the steady-state photocurrent under monochromatic light at 530 nm, along with the temperature-dependent mobility measured on a field-effect transistor constructed on a 6T single crystal.

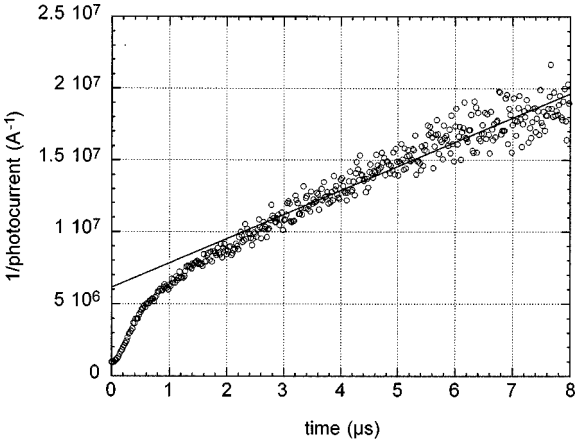

FIG. 9. Variation of the reversed photocurrent as a function of time. Data are taken from Fig. 4. The solid line is a linear least-squares fit to the data at times greater than 2 μs.

$$I_{\mathrm{ph}}=Wd_{\mathrm{eff}}nq(\mu_+ +\mu_-)\frac{V}{L}. \tag{4}$$

Here, q is the electron charge, μ_+ and μ_- are the mobility of the positive and negative charges, respectively, V is the applied voltage, and L is the interelectrode distance. We assume that the electric field F is uniform all over the crystal, which seems reasonable owing to the magnitude of the interelectrode distance, so that $F=V/L$. We have also verified the strict linearity of the photocurrent with the applied voltage, both in the time-resolved and steady-state measurements.

$1/I_{\mathrm{ph}}$ as a function of t is plotted in Fig. 9. For a Langevin-type recombination process,[12] the recombination coefficient is given by Eq. (5), where ε is the permittivity of the material,

$$\gamma=\frac{q(\mu_+ +\mu_-)}{\varepsilon}. \tag{5}$$

Inserting Eqs. (4) and (5) in Eq. (3), we get

$$\frac{1}{I_{\mathrm{ph}}}=\frac{L}{Wd_{\mathrm{eff}}q(\mu_+ +\mu_-)n(0)V}+\frac{L}{Wd_{\mathrm{eff}}\varepsilon V}t. \tag{6}$$

From the slope of the fitted straight line in Fig. 9 and the geometrical dimensions of the crystal ($L=2$ mm, $W=3$ mm), we find $d_{\mathrm{eff}}=20\ \mu$m, which is not too far from the actual thickness of the crystal (12 μm). (We took $\varepsilon/\varepsilon_0=3$, where ε_0 is the permittivity of vacuum.) This suggests that the effective thickness corresponds to the actual thickness of the crystal, which would in turn mean that the time taken by the carriers to diffuse over the whole thickness of the crystal is short as compared to time scale of the measurement.

The photocarrier density at $t=0$ can be estimated from the extrapolation of the straight line to the y axis. For this, we assume that the mobility of holes largely exceeds that of electrons, so that $\mu_+ +\mu_- \approx \mu_+$, and take for the former a magnitude of 0.1 $\mathrm{cm^2\,V^{-1}\,s^{-1}}$, as reported from field-effect measurements on sexithiophene single crystals;[10,11] we get $n(0)\approx 10^{13}\,\mathrm{cm^{-3}}$. The number of initial photocarriers is obtained by multiplying this density by the active volume of the crystal, that is, that included between the electrodes

$(0.2\times0.3\times0.001\,\mathrm{cm}^3)$; we get 6×10^8 carriers. The energy of the laser pulse was estimated to $10\pm5\,\mu$J, which corresponds to $(2\pm1)\times10^{13}$ photons. We therefore estimate that the initial quantum efficiency for carrier generation η ranges between 2×10^{-5} and 6×10^{-5}.

We now turn to the first component of the slow decay. As stated above, the large load resistance used to detect it probably widens this component. However, it is still too long to be ascribed to the fast component. A trapping mechanism can be excluded since the photocurrent decay remains bimolecular all along; one would have to imagine a perfectly symmetrical trapping of electrons and holes, which is most unlikely. We therefore tentatively attribute this intermediate component to *geminate* recombination of the excitons, as opposed to recombination of well-separated electrons and holes in the second component of the slow decay. Note that the presence of geminate recombination would suggest that the photocarrier quantum efficiency had been underestimated, which seems in agreement with the data obtained from steady-state measurements, as will be shown in the following.

Turning now to the steady-state photoconductivity, Eq. (1) becomes

$$G-\gamma(n_0+n)n=0 \tag{7}$$

which can be resolved to

$$n=\frac{n_0}{2}\left[\left(1+\frac{4G}{\gamma n_0^2}\right)^{1/2}-1\right]. \tag{8}$$

Making use of Eq. (4), where we substitute the effective thickness by the actual thickness d of the crystal, and noting that $G=\eta\Phi_0/d$, where Φ_0 is the photon flux, the photocurrent is given by Eq. (9). We account here for the fact that, as shown above, the time taken by the photocarriers to diffuse over the entire thickness of the crystal (less than 1 μs) is much shorter than that taken to measure the photocurrent, 10 ms,

$$I_{\mathrm{ph}}=\frac{Wdn_0q(\mu_++\mu_-)V}{2L}\left[\left(1+\frac{4\eta\Phi_0}{\gamma n_0^2 d}\right)^{1/2}-1\right]. \tag{9}$$

The solid line in Fig. 7 is a least-squares fit of the data to Eq. (9). We get $n_0=10^{11}\,\mathrm{cm}^{-3}$, in excellent agreement with values obtained from field-effect measurements.[10] Also note that the magnitude of n_0 is indeed much lower than that of the initial density of photocarriers in the time-resolved measurements. Next, we get an initial quantum yield of 2×10^{-4}, which is slightly less than ten times higher than that estimated from the time-resolved photoconductivity. As stated above, this slight discrepancy could be attributed to geminate recombination. At this point, we have therefore established that the primary generation of photocarriers occurs with a quantum yield of around 10^{-4}, and that the slow decay corresponds to a bimolecular recombination of electrons and holes according to a Langevin mechanism.

In order to analyze the short-lived photocurrent (Fig. 5), we will refer to a procedure developed by Yacoby and co-workers,[13,14] which involves an estimation of the carrier migration distance l from Eq. (10), where N_e and N_{ph} are the number of collected charge and absorbed photons, respectively, and η_0 is the primary quantum efficiency for carrier generation,

$$\frac{N_e}{N_{\mathrm{ph}}}=\eta_0 l/L. \tag{10}$$

N_e is estimated from the integration of the photocurrent in Fig. 5 (about 3 pC). This analysis rests on the fact that in a pulsed photoconductivity experiment on a nanosecond time scale, only carrier drift along the molecule or to its nearest neighbors can be observed. Assuming a unity quantum yield, we get an upper limit of the drift length of around 2 nm. Note that the charge drift occurs *along* the crystal plane. Since this drift length exceeds the lattice parameters in that plane [0.79 and 0.60 nm (Ref. 6)], charges are necessarily transferred between neighboring molecules during the fast initial process. We therefore attribute the initial decay to the conversion of charge-transfer excitons (localized over adjacent molecules) to molecular excitons.

The similarity between the photoluminescence and photocurrent action spectra indicates that charge generation occurs through dissociation of excitons. Because of the low electric field involved (5000 V/cm at most), we can exclude an electric field assisted mechanism, and assume a thermally activated process, which would occur according to Eq. (11),

$$M^*\leftrightarrow M^++e^-. \tag{11}$$

Here, M^*, M^+, and e^- are an exciton (excited molecule) and a photogenerated hole and electron, respectively. From simple mass action law, the respective densities of photocarriers (n) and excitons (n^*) are related by Eq. (12), where we account for the fact that holes and electrons are produced in equal amount,

$$\frac{n^2}{n^*}=\kappa\exp\left(-\frac{E_b}{kT}\right). \tag{12}$$

Here, κ is a temperature-independent constant. The minus sign in the exponential mirrors the fact that reaction (11) is more favorable from right to left. In other words, the exciton is more stable than two separate charges. The photocurrent quantum yield results in two sequential mechanisms, namely the formation of excitons and the splitting of the excitons into charges. Because the rate of exciton generation can be reasonably assumed to be close to 1 and temperature independent, we see that $\eta\propto\exp(-E_b/2kT)$. We can further set the prefactor to 1 simply because the quantum yield is expected to approach unity as the exciton binding energy approaches zero. Taking into account the extreme magnitude of the quantum yield, $2\times10^{-5}<\eta<2\times10^{-4}$, we obtain an exciton binding energy $E_b=0.50\pm0.06\,\mathrm{eV}$, in good agreement with the estimation by Taliani and Blinov[8] (see the Introduction). Note that, because of the logarithm dependence of E_b with the quantum yield, an error by one order of magnitude in the latter only leads to a 10% error in the former. This estimation is confirmed by the temperature-dependent measurements. Both the photocurrent and the mobility of $6T$ are found to be thermally activated with respective activation energies 0.30 ± 0.05 and 0.05 ± 0.01 eV. From Eq. (4) we see that the activation energy of the quantum yield equals that of

the photocurrent minus that of the mobility. This leads to a binding energy 0.50 ± 0.10 eV, in excellent agreement with that deduced from the magnitude of the quantum yield at room temperature.

As a final remark, we note that, in contrast with an earlier report,[15] we do not observe any increase of the steady-state photoconductivity beyond 3 eV, where charge-transfer excitons, rather than molecular excitons, are likely to form. As stated above, this is due to the fast decay of the CTE's into molecular excitons, as indicated by the fast component of the time-resolved photoconductivity.

CONCLUSION

We have carried out steady-state and time-resolved photocurrent measurements on sexithiophene single crystals at low applied electric field. The photocurrent action spectrum coincides with that of the photoluminescence excitation, which indicates that photocarriers originate from a splitting of molecular excitons. Two features can be discerned in the time-resolved photoconductivity: first, a fast response, with a decay time lower than 1 ns, which we attribute to the deactivation of charge-transfer excitons into molecular excitons; next, a slow decay that can be in turn divided into two components, a faster one, which we tentatively attribute to geminate recombination of the molecular excitons, followed by a second-order decay, which is ascribed to the bimolecular recombination of well-separated electrons and holes. The dependence of the steady-state photocurrent as a function of light illumination also supports this picture. We estimate an initial quantum efficiency ranging between 2×10^{-5} and 2×10^{-4}, the low magnitude of which is in favor of a thermally assisted process, and a concentration of carriers at equilibrium of $10^{11}\,\mathrm{cm}^{-3}$, in good agreement with previous evaluations from field-effect measurements.[10] From the quantum efficiency, we estimate an exciton binding energy of 0.50 ± 0.06 eV. This value is confirmed by the temperature dependence of the photocurrent.

ACKNOWLEDGMENTS

This work has been partly supported by the European Union Training and Mobility for Researchers program on Synthetic Electroactive Organic Architecture (SELOA).

*Electronic address: horowitz@glvt-cnrs.fr

[1] M. Pope and C. E. Swenberg, *Electronic Processes in Organic Crystals* (Oxford University Press, New York, 1982).
[2] S. Barth and H. Bässler, Phys. Rev. Lett. **79**, 4445 (1997).
[3] A. J. Heeger, in *Primary Photoexcitations in Conjugated Polymers: Molecular Exciton Versus Semiconductor Band Model*, edited by N. S. Sariciftci (World Scientific, Singapore, 1997).
[4] S. Barth, H. Bässler, H. Rost, and H. H. Horhold, Phys. Rev. B **56**, 3844 (1997).
[5] D. Moses, J. Wang, G. Yu, and A. J. Heeger, Phys. Rev. Lett. **80**, 2685 (1998).
[6] G. Horowitz, B. Bachet, A. Yassar, P. Lang, F. Demanze, J. L. Fave, and F. Garnier, Chem. Mater. **7**, 1337 (1995).
[7] M. Muccini, E. Lunedei, A. Bree, G. Horowitz, F. Garnier, and C. Taliani, J. Chem. Phys. **108**, 7327 (1998).
[8] C. Taliani and L. M. Blinov, Adv. Mater. **8**, 353 (1996).
[9] C. H. Lee, G. Yu, D. Moses, and A. J. Heeger, Phys. Rev. B **49**, 2396 (1994).
[10] G. Horowitz, F. Garnier, A. Yassar, R. Hajlaoui, and F. Kouki, Adv. Mater. **8**, 52 (1996).
[11] G. Horowitz, R. Hajlaoui, and F. Kouki, Eur. Phys. J.: Appl. Phys. **1**, 361 (1998).
[12] P. Langevin, Ann. Chim. Phys. **28**, 433 (1903).
[13] Y. Yacoby, S. Roth, K. Menke, F. Keilmann, and J. Kuhl, Solid State Commun. **47**, 869 (1983).
[14] D. C. C. Bradley, Y. Q. Shen, H. Bleier, and S. Roth, J. Phys. C **21**, L515 (1988).
[15] G. Horowitz, S. Romdhane, H. Bouchriha, P. Delannoy, J. L. Monge, F. Kouki, and P. Valat, Synth. Met. **90**, 187 (1997).